# Study on Rough-Surface Biaxially Oriented Polypropylene Film. V. Analysis and Control of Roughness

MITSUYOSHI FUJIYAMA, YOSHIMASA KAWAMURA, and TETSUO WAKINO, *Polymer Development Laboratory, Tokuyama Soda Co., Ltd., Tokuyama-shi, Yamaguchi-ken 745, Japan,* and TOMOMI OKAMOTO, *Printed Circuit Products, Electronic Business Division, Tokuyama Soda Co., Ltd., Fujisawa-shi, Kanagawa-ken 252, Japan*

## Synopsis

In the previous papers, the roughening of biaxially oriented polypropylene film (BOP) by utilizing β-form crystals in a successively stretching tenter method has been studied, and BOPs with various roughness have been obtained. In the present paper, the results obtained in the previous studies have been summarized. The roughness can quantitatively be represented by average roughness $R_a$ (depth of roughness) and roughness period $L$ (density of roughness). $R_a$ and $L$ can largely be changed by changing machine direction (MD)-stretching temperature and the melt flow index (MFI) of base polypropylene (PP), respectively. Furthermore, a BOP with a low roughness period (high density of roughness) can be obtained by adding crystal nucleators to the base PP.

## INTRODUCTION

In the previous studies[1-4] on the roughening of biaxially oriented polypropylene film (BOP) by utilizing β-form crystals in a successively stretching tenter method, BOPs with various roughness have been obtained by selecting the melt flow index (MFI) of base polypropylene (PP),[3] crystal nucleator content,[4] casting conditions of sheet,[2] and machine direction (MD)- and transverse direction (TD)-stretching conditions.[2-4] In the present study the roughness of these BOPs has been analyzed and a quantitative representation of the roughness has been tried.

Next, the relations between various factors and the roughness have been analyzed, and the control of the roughness has been studied.

Last, the relations between the roughness and the practical properties such as impregnation properties of insulating oils and dielectric breakdown strength have been studied.

## METHOD OF ANALYSIS

### Analysis of Roughness

In order to quantify roughness, average roughness $R_a$ and maximum roughness $R_m$, which represent the depth of roughness and roughness period $L$, which represents the density of roughness, were evaluated. Since the

Journal of Applied Polymer Science, Vol. 36, 1035–1048 (1988)
 CCC 0021-8995/88/051035-14$04.00

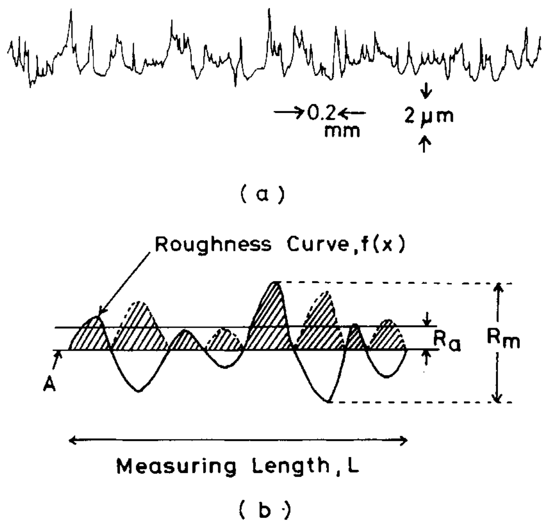


Fig. 1. (a) An example of roughness curve, $f(x)$, of a rough-surface BOP. (b) Schematic representation of roughness curve for explanation of average roughness $R_a$ and maximum roughness $R_m$.

roughness was craterlike, the diameter of the craters, $D$, and the density of the craters, $d$, were also evaluated.

**Average Roughness $R_a$ (JIS B0601).** Figure 1(a) shows an example of the roughness curve $f(x)$ of a rough-surface BOP which was measured with a Surfcorder Model TDF-3A manufactured by Kosaka Laboratory Ltd. Figure 1(b) shows a model of the roughness curve. A center line $A$ is drawn on the curve, and $R_a$ is calculated by integrating the shadowed parts and by dividing the integrated value by the measuring length $l$:

$$R_a = \frac{1}{l}\int_0^l |f(x)|\, dx$$

The measurement of $R_a$ was carried out five times along the MD of BOP with $l$ of 16 mm and the average value was adopted.

**Maximum Roughness $R_m$ (JIS B0601).** The distance between the highest peak and the lowest valley of the roughness curve shown in Figure 1(b) is regarded as $R_m$. The measurement of $R_m$ was carried out five times along the MD of the BOP with $l$ of 10 mm and the average value was adopted.

**Roughness Period $L$.** A period in which a roughness higher than $R_m/3$ appeared was regarded as roughness period $L$. The number of the roughness higher than $R_m/3$, $N$, was measured in a measuring length of 5 cm, and $L$ was calculated by the following equation:

$$L = \frac{5 \times 10^3}{N}$$

**Crater Diameter $D$.** The diameter of the craters on a rough-surface BOP was measured from its surface photograph. The average value of the major diameter and the minor diameter was adopted as $D$.

**Crater Density *d*.** The number of the craters per 1 $cm^2$, $d$, on a rough-surface BOP was measured from its surface photograph.

### Control of Roughness

The relations between the factors which influence the roughening of BOP and $R_a$ and $L$ which represent the roughness were studied. The factors studied were as follows: (i) MFI of base PP[3]; (ii) content of $\alpha$-crystal or $\beta$-crystal nucleator[4]; (iii) casting conditions of sheet[4]; (iv) MD-stretching temperature[2-4]; (v) TD-stretching temperature.[3]

### Relations between Roughness and Properties

The roughening of BOP is conducted mainly in order to improve the impregnation properties of insulating oils of the BOP. The relations between the impregnation properties and the roughness were studied by the method described later. Since it was apprehended that the dielectric breakdown strength of BOP might be reduced by the roughening, the relation between the dielectric breakdown strength and the roughness was also studied.

## RESULTS AND DISCUSSION

### Analysis of Surface State

As factors which represent a surface state, the average roughness $R_a$ the maximum roughness $R_m$, the roughness period $L$, the crater diameter $D$, and the crater density $d$ were evaluated and analyzed for various rough-surface BOPs obtained so far. These factors are roughly divided into two groups: $R_a$ and $R_m$, which represent the depth of the roughness, and $L$, $D$, and $d$, which represent the density of the roughness. $R_a$ and $R_m$ out of these factors are in a proportional relationship to each other, and $R_m$ is about 10 times of $R_a$ as shown in Figure 2. Accordingly, $R_a$ can be used as a representative of the factors which represent the depth of the roughness.

Next, as for the factors which represent the density of the roughness, the relation between $D$ and $L$ and the relation between $d$ and $L$ are shown in Figures 3 and 4, respectively. $D$ and $L$ are in a proportional relationship with a slope of about 0.8 except for the two points with high $L$. $d$ and $L$ are in a linear relationship with a slope of about $-2$ when plotted double logarithmically. These facts are theoretically reasonable: When the crater diameter $D$ increases to an extent, the frequency of the flange of the crater decreases to that extent, and hence the roughness period $L$ necessarily increases to that extent. And, since the crater density $d$ is the number of craters per unit area, when $d$ increases $n$ times, the number of the flanges of the craters per unit length increases $n^{-1/2}$ times, and hence the roughness period $L$ should also increase $n^{-1/2}$ times. Thus, when $d$ and $L$ are plotted double logarithmically, a linear relationship with a slope of $-2$ should be obtained. Since the factors which represent the density of the roughness are in correlationships with one another, they can be represented by the roughness period $L$ as a representative.

The roughness states of the BOPs obtained so far are shown in Figure 5 using $R_a$ and $L$ as representatives. It can be seen from Figure 5 that the BOPs with various roughness have been obtained so far.

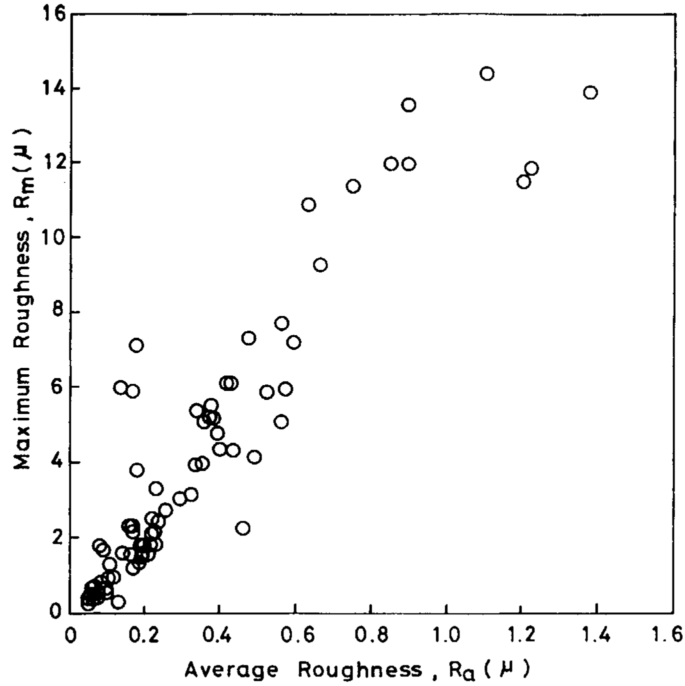


Fig. 2. Relation between maximum roughness $R_m$ and average roughness $R_a$.

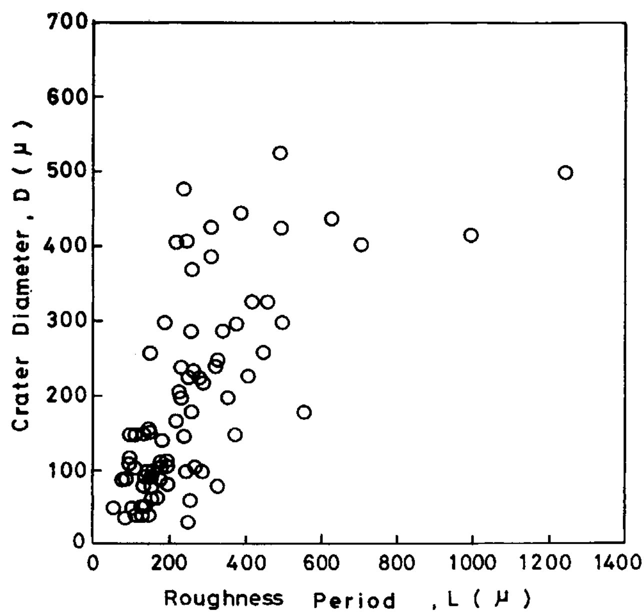


Fig. 3. Relation between crater diameter $D$ and roughness period $L$.

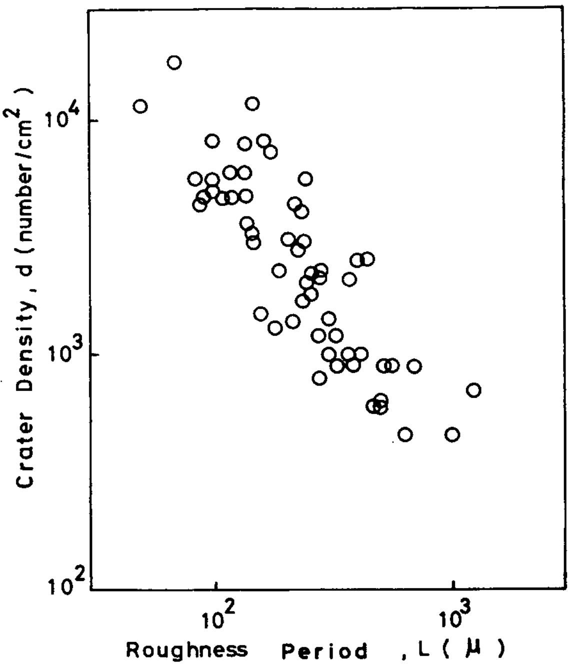


Fig. 4. Relation between crater density $d$ and roughness period $L$.

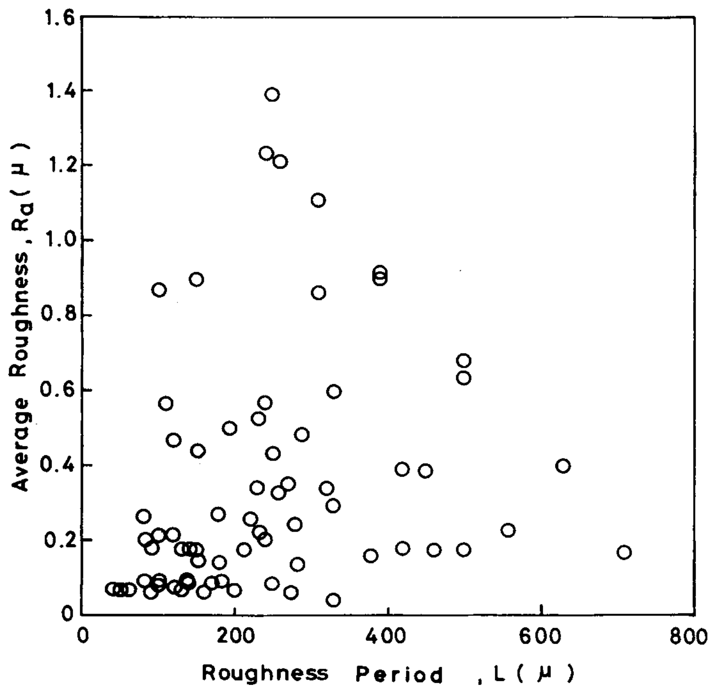


Fig. 5. Map of average roughness $R_a$ vs. roughness period $L$ for rough-surface BOPs made in our laboratory.

## Control of Roughness

**MFI of Base PP.** The relation between the MFI of base PP and the amount of $\beta$-crystals formed in the cast sheet obtained from it has been studied,[3] and it has been found that the amount of the $\beta$-crystals was maximum at MFI $\doteqdot$ 8 dg/min. Then, the relation between the MFI of the base PP and the roughness of the BOP obtained from it was studied, and the results are shown in Figure 6. With increasing MFI, $L$ decreases largely, and $R_a$ does not change so much. By adjusting the MFI of the base PP, the surface state can be controlled in ranges of $R_a$ = 0.7–0.9 $\mu$m and $L$ = 1200–400 $\mu$m.

**Addition of α-Crystal or β-Crystal Nucleator.** As for the influence of the addition of crystal nucleators, with increasing nucleator content, the diameter of the $\beta$-spherulites in the cast sheet decreases, and the diameter of the craters and $R_a$ of the BOP obtained from it decrease in proportion to it in both the cases of $\alpha$- and $\beta$-nucleators, as shown in the Part IV of this series.[4] Figure 7 shows the relation between the diameter of the $\beta$-spherulites in the cast sheet and that of the craters on the BOP obtained from it. The both are in a proportional relationship, and so the diameter of the craters on a BOP is determined almost by the nucleator content.

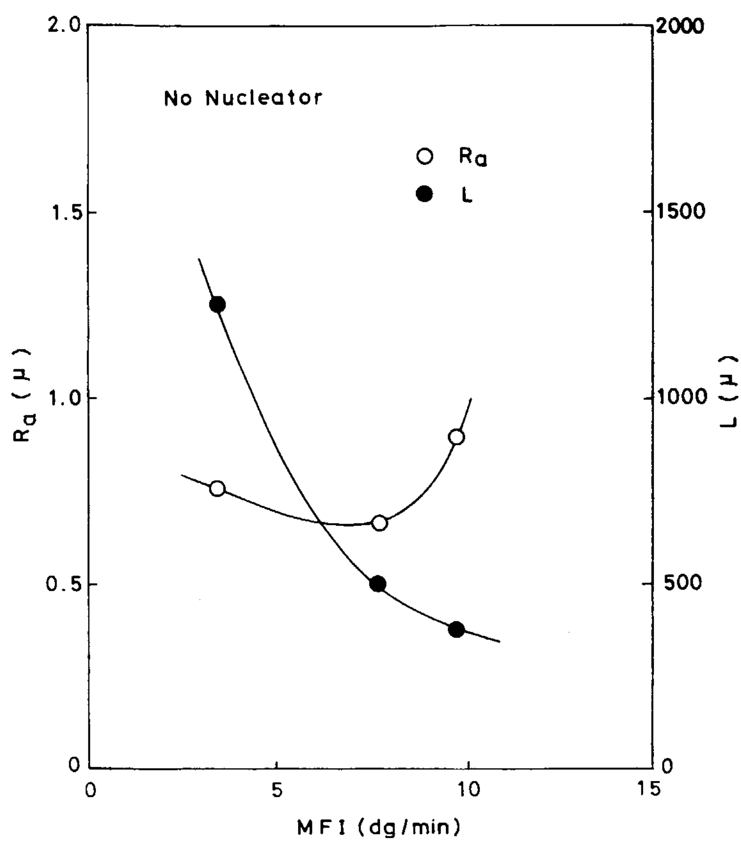


Fig. 6. Influence of MFI of PP resin with no nucleator on roughness of BOP: (○) $R_a$; (●) $L$.

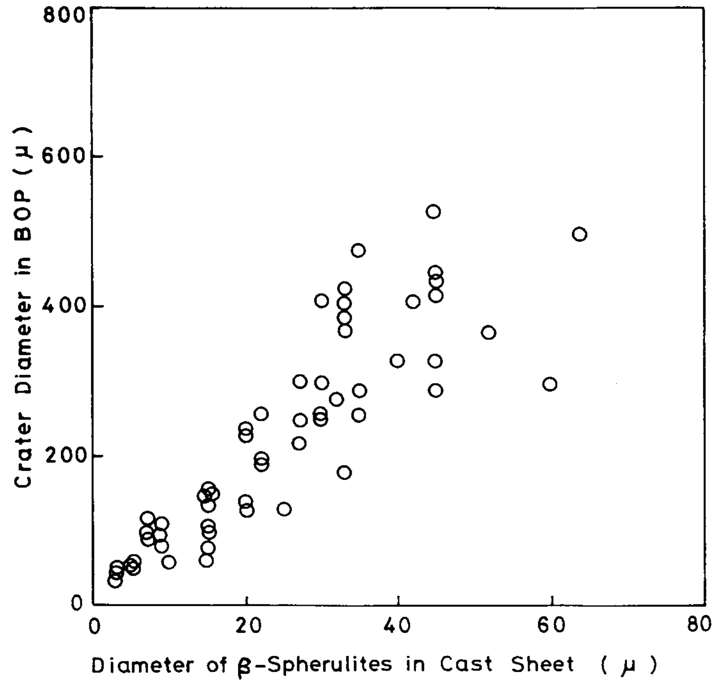


Fig. 7. Relation between diameter of craters on BOP and diameter of β-spherulites in cast sheet.

Figure 8(a) shows the relation between the α-nucleator content in the base PP and the roughness of the BOP obtained from it. With increasing α-nucleator content, $R_a$ decreases largely and $L$ does not change so much. The amount and diameter of the β-spherulites formed in the cast sheet tend to decrease with increasing α-nucleator content.[4] Consequently, both the number and diameter of the craters on the BOP obtained from it decrease with increasing α-nucleator content, the effect of the decrease in the number on $L$ and that in the diameter on $L$ cancel each other, and hence $L$ does not change so much.

Figure 8(b) shows the relation between the β-nucleator content in the base PP and the roughness of the BOP obtained from it. Both $R_a$ and $L$ tend to decrease with increasing β-nucleator content. In the case of the β-nucleator, differing from the case of the α-nucleator, the amount and diameter of the β-spherulites formed in the cast sheet tend to, respectively, increase and decrease with increasing β-nucleator content.[4] Consequently, the number and diameter of the craters on the BOP obtained from it, respectively, increase and decrease with increasing β-nucleator content, and hence $L$ decreases.

**Casting Conditions of Sheet.** Figures 9(a) and (b) show the influences of, respectively, the extrusion temperature and the chill roll temperature at the time of casting sheet on the roughness of the BOP obtained from it. With decreasing extrusion temperature, the amount of the β-spherulites increases,[1,2] and hence $R_a$ increases. With increasing chill roll temperature, the amount of the β-spherulites increases,[1] and hence $R_a$ increases. As for $L$, since the BOPs in Figure 9 were obtained from the base PPs with no nucleator, the diameters

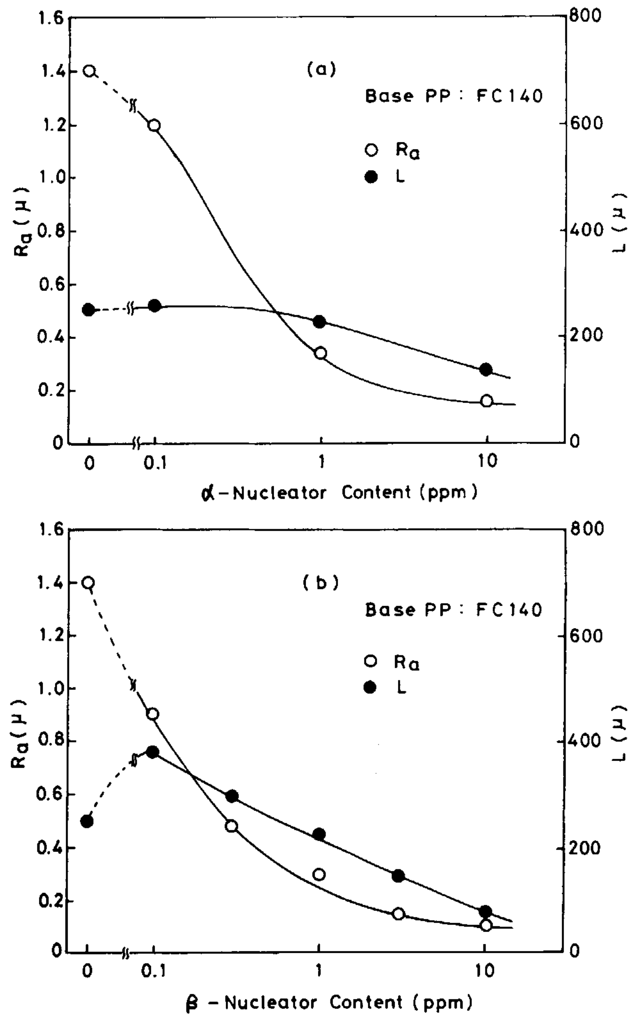


Fig. 8. Influences of (a) α-nucleator content and (b) β-nucleator content in PP resin on roughness on BOP: (○) $R_a$; (●) $L$.

of the craters on them are very large, $L$'s are generally high, and the correlationship between the casting conditions of the sheet and $L$ is not clear. However, taking the amount of the β-spherulites formed in the cast sheet into consideration, it is desirable to cast the sheet a low extrusion temperature and a high chill roll temperature.

**MD-Stretching Temperature.** Figure 10 shows the influence of the surface temperature of the MD-stretching roll on the roughness of the BOP. $R_a$ increases largely with increasing MD-stretching temperature. On the other hand, $L$ does not change so much by changing the MD-stretching temperature. Namely, by changing the MD-stretching temperature, the depth of roughness changes largely and the density of roughness does not change so much. BOPs with good surface state were obtained at MD-stretching temperatures around 140°C.

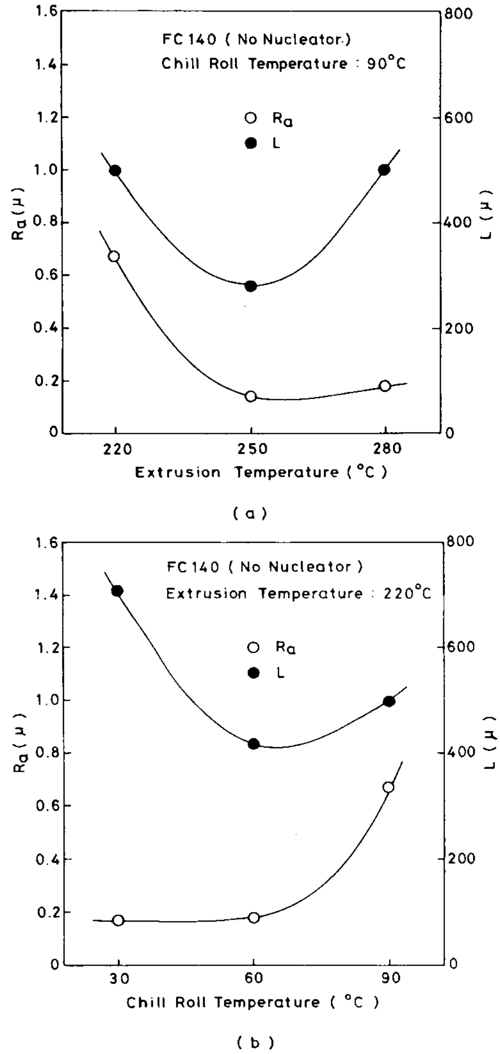


Fig. 9. Influences of (a) extrusion temperature and (b) chill roll temperature of cast sheet on roughness of BOP: (○) $R_a$; (●) $L$.

**TD-Stretching Temperature.** Figure 11 shows the influence of the TD-stretching temperature on the roughness of BOP. The TD-stretching was carried out at a temperature range of 145–158°C. $R_a$ and $L$ tend to increase with decreasing TD-stretching temperature. However, when the TD-stretching temperature is too low, the possibility of forming nonuniform roughness is high.[3] On the other hand, at high TD-stretching temperatures, both $R_a$ and $L$ are low. When the TD-stretching is performed at too high temperatures, the craters on the BOP have been melted, and the roughness state is not good.[3] Consequently, the degree of the roughness, $R_a$, is not so high and the period of roughness, $L$, is comparatively low. Since the roughening of BOP is achieved in the MD-stretching process by utilizing the difference of the stretching behaviors of the $\beta$- and $\alpha$-crystals and the TD stretching is applied

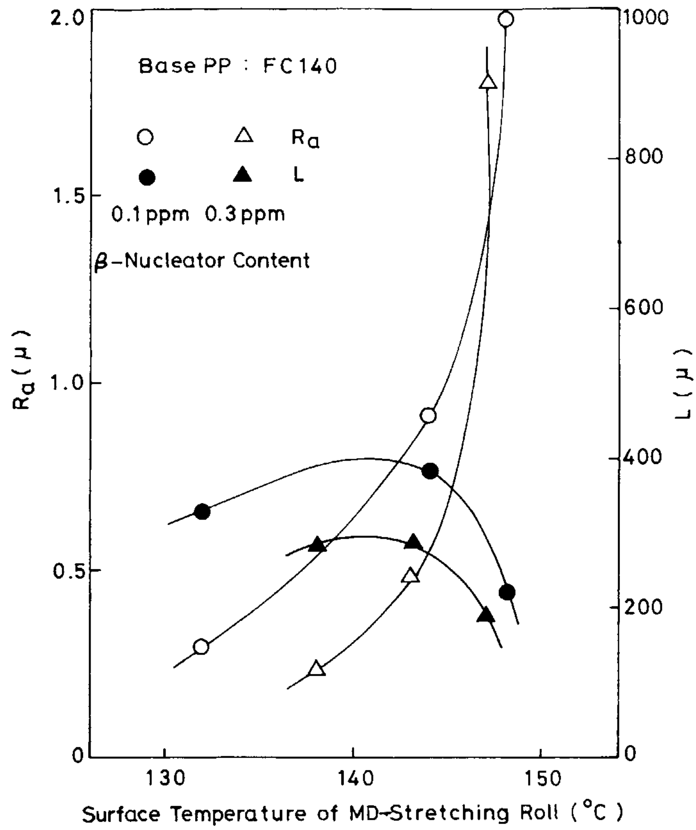


Fig. 10. Influence of surface temperature of MD-stretching roll on roughness of BOP: (○, △) $R_a$; (●, ▲) $L$; (○, ●) 0.1 ppm; (△, ▲) 0.3 ppm.

only to extend the rough surface formed in the MD-stretching process to the TD,[2] it is enough to select the temperature range where the stretching is performed uniformly and effectively. Accordingly, TD-stretching temperatures around 150°C are suitable.

The factors affecting the roughness of BOP discussed above are summarized in Figure 12. When controlling the roughness of BOP, rough values of $R_a$ and $L$ are first set by selecting the MFI and α-crystal or β-crystal nucleator content of the base PP, and the value of $R_a$ is next determined by adjusting the MD-stretching temperature.

## Relations between Roughness and Properties

**Impregnation Properties of Insulating Oils.** Since there is no term for evaluating the impregnation properties of insulating oils of plastic films for the capacitor in JIS or ASTM, they were evaluated according to the Mitsubishi Rayon method.[5] As shown in Figure 13, a film was tightly wound two times so that the rough surface faced outside on a glass tube with a diameter of 5 cm and a length of 15 cm which was stood on a share filled with an insulating oil, and the time change of the height of the oil which rose between the films was measured at 23°C. The insulating oil used was a capacitor oil S

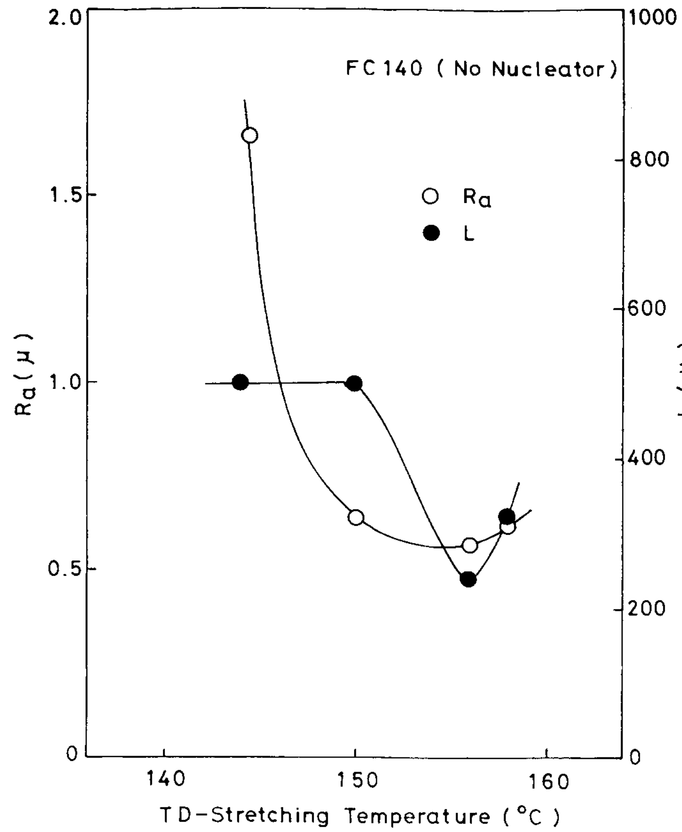


Fig. 11. Influence of TD-stretching temperature on roughness of BOP: (○) $R_a$; (●) $L$.

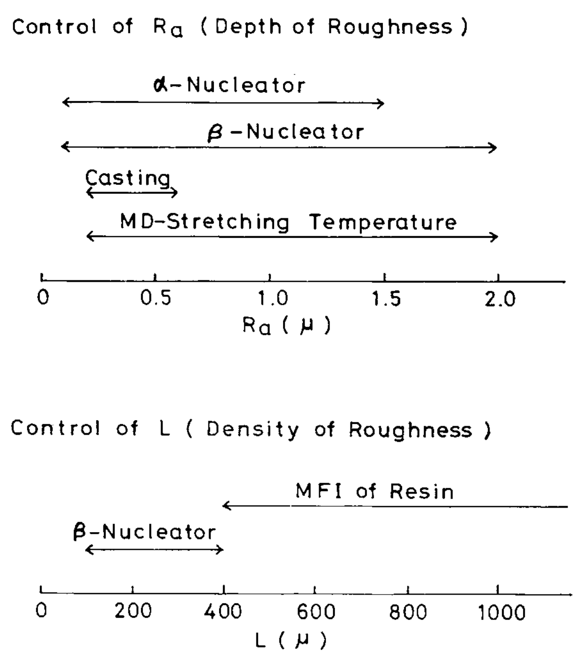


Fig. 12. Control of surface roughness of BOP.

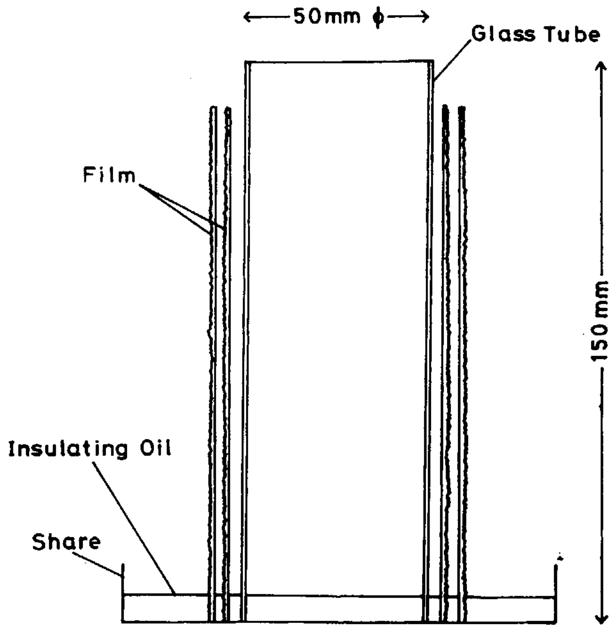


Fig. 13. Apparatus for measurement of impregnation rate of insulating oil.

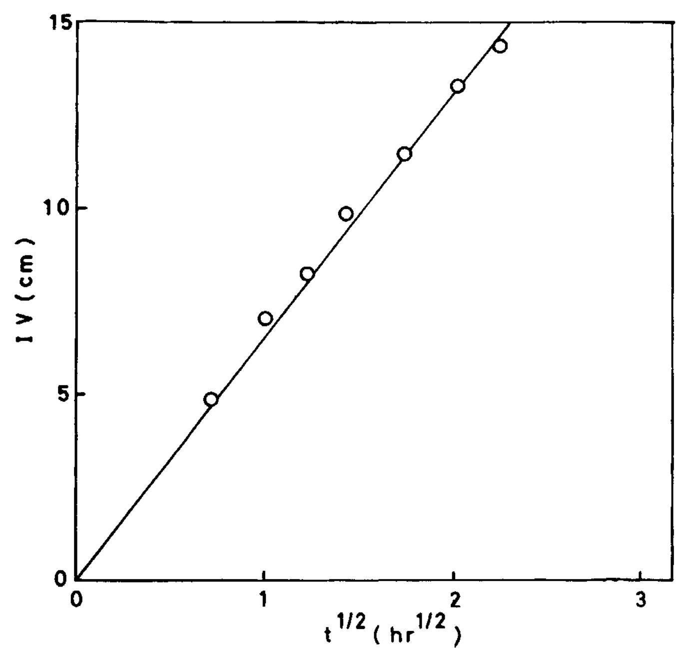


Fig. 14. Plot of impregnation value IV vs. root of time for a rough-surface BOP.

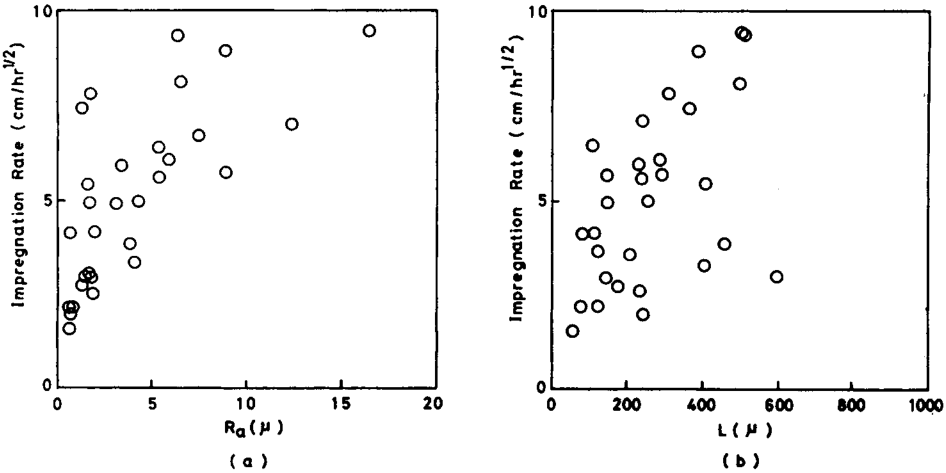


Fig. 15. Relations between impregnation rate of insulating oil and (a) average roughness $R_a$ and (b) roughness period $L$ of BOP.

(PXE; phenyl xylyl ethane) produced by Nihon Sekiyukagaku Kogyo Co., Ltd. The IV (impregnation value), which is the height of the oil, is given by the following equation:

$$\text{IV} \propto \sqrt{TD\cos\theta t/3\mu}$$

where $T$ is the surface tension of the oil, $D$, the distance between films, $\theta$, the contact angle, $\mu$, the viscosity of the oil, and $t$, time. Accordingly, IV is proportional to $t^{1/2}$, and a linear relationship is obtained when IV is plotted against $t^{1/2}$. Figure 14 shows an example of these plots. The slope of this line was regarded as an impregnation rate. At the same time, the impregnated states such as the remainder of voids were observed.

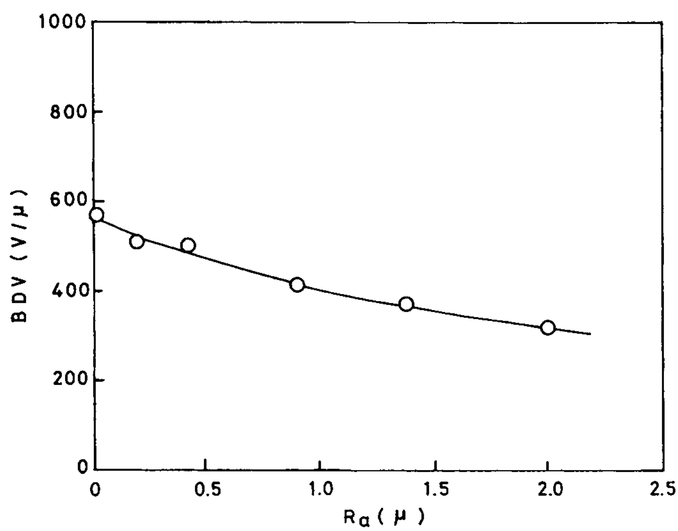


Fig. 16. Dependence of dielectric breakdown voltage BDV on average roughness $R_a$.

Figures 15(a) and (b) show the relations between the impregnation rate and $R_a$ and $L$, respectively. Although it seems that there are weak trends that the impregnation rate tend to increase with increasing $R_a$ and $L$, the trends are not so clear. The voids tend to remain and the impregnated state was not good when $R_a$ was above about 0.5 $\mu$m.

**Dielectric Breakdown Strength.** The dependence of the dielectric breakdown voltage (BDV) per unit thickness of BOP measured under direct current with a dielectric breakdown strength measuring apparatus Type KD-103AD-X-I manufactured by Toyo Seiki Seisakusho Co., Ltd., according to the JIS C2330 upon $R_a$, is shown in Figure 16. BDV gradually decreases with increasing $R_a$. Accordingly, a BOP with too high $R_a$ is not favorable when viewed from electric properties.

## CONCLUSIONS

The roughness of the BOPs obtained so far was analyzed, and it was quantified by the use of the average roughness $R_a$, which represents the depth of the roughness, and the roughness period $L$, which represents the density of the roughness. As the result, it became clear that BOPs with various roughness could be obtained by appropriately selecting the base resin and the processing conditions.

As for the control of the roughness, $R_a$ and $L$ can be changed largely by appropriately selecting the MD-stretching temperature and the MFI of the base PP, respectively. Furthermore, by adjusting the $\alpha$- or $\beta$-nucleator content, the diameter of the craters on BOP can be controlled and a BOP with a high density of craters can be obtained.

As for the relations between the roughness and the properties of BOP, taking the impregnation properties of insulating oils and the dielectric breakdown strength into consideration, practically favorable BOPs are the ones with $R_a \doteqdot 0.5$ $\mu$m and $L \leq 300$ $\mu$m. Such BOPs can be obtained by using the base PP with a high MFI (about 8 dg/min) and an appropriate amount (about 1 ppm) of $\alpha$- or $\beta$-nucleator and by MD stretching at high temperatures (roll surface temperature of about 145°C).

## References

1. M. Fujiyama, Y. Kawamura. T. Wakino, and T. Okamoto, *J. Appl. Polym. Sci.*, **36**, 985 (1988).
2. M. Fujiyama, Y. Kawamura, T. Wakino, and T. Okamoto, *J. Appl. Polym. Sci.*, **36**, 995 (1988).
3. M. Fujiyama, Y. Kawamura, T. Wakino, and T. Okamoto, *J. Appl. Polym. Sci.*, **36**, 1011 (1988).
4. M. Fujiyama, Y. Kawamura, T. Wakino, and T. Okamoto, *J. Appl. Polym. Sci.*, **36**, 1025 (1988).
5. Mitsubishi Rayon Co., Ltd., Mirayphan SX® Technical Data.

Received August 11, 1987
Accepted November 7, 1987